

# The stability of DNA triplexes inside cells as studied by iodine-125 radioprinting

Olga A. Sedelnikova, Igor G. Panyutin\*, Andrew N. Luu and Ronald D. Neumann

Department of Nuclear Medicine, Warren G. Magnuson Clinical Center, National Institutes of Health, Bethesda, MD 20892, USA

Received June 8, 1999; Revised and Accepted August 9, 1999

## ABSTRACT

We studied the stability of a DNA triplex resulting from the binding of a 38 nt long purine motif triplex-forming oligonucleotide (TFO) to a covalently closed plasmid containing a target sequence from the human HPRT gene. Our *in vitro* experiments showed that the triplex formed at plasmid and TFO concentrations as low as  $10^{-9}$  M. Once formed, the triplex was remarkably stable and could withstand 10 min incubation at 65°C. We next delivered these TFO–plasmid complexes into cultured human cells. To monitor the TFO–plasmid complexes inside cells we applied a new technique that we call ‘radioprinting’. Because the TFO was  $^{125}\text{I}$  labeled, we could quantitatively monitor the triplexes by measuring  $^{125}\text{I}$ -induced DNA strand breaks in the target plasmid sequence. We found that the triplexes remain stable inside the cells for at least 48 h. Based on these findings we propose using TFO for indirect labeling of intact plasmid DNA. As a demonstration, we show that the intracellular distribution of a fluorescein-labeled TFO was different when it was liposome-delivered into cultured human cells alone or in a complex with the plasmid. In the latter case, the fluorescence was detected in nearly all the cells while detection of the plasmid by use of a marker gene ( $\beta$ -galactosidase) revealed expression of the gene in only half of the cells.

## INTRODUCTION

Short synthetic oligodeoxyribonucleotides can bind complementary polypurine-polypyrimidine sequences in a sequence-specific manner by forming triple helices (or triplexes) in the major groove of the DNA duplex (reviewed in 1,2). Such triplex-forming oligonucleotides (TFOs) provide a unique opportunity for the rational design of DNA sequence-specific drugs and have been proposed for use in regulation of gene expression *in vivo* (reviewed in 3). Regardless of numerous attempts to improve the stability and the DNA binding properties of TFOs *in vivo* much remains to be done before clinical applications become a reality. The main obstacle is that DNA in the eukaryotic nucleus is tightly packed into chromatin, which may limit access of TFOs to their targets.

The thermodynamics and kinetics of triplex formation with purified DNA have been intensively studied (reviewed in 4). Stability of triplexes has been shown to be sequence dependent (2). However, the exact rules that would allow prediction of the stability of a triplex based on its sequence are not yet established. The stability of triplexes can be improved with certain chemical modifications of the TFO bases and the backbone (reviewed in 5,6).

An effect of TFOs on gene expression was demonstrated in several studies (3,6) and triplex formation was shown inside permeabilized cells (7–9). TFOs have been found to cause gene-specific mutations (10,11), although the yield of mutants was too low to account for the effects of TFO on gene expression. Still, there is no direct evidence that TFOs bind their targets in live cells. The main reason for this is the lack of a simple and reliable method of detection of triplex formation inside cells. Development of such a method would allow efficient selection of the best sequence motif and bases/backbone modification of TFOs for a target sequence inside cells as well as provide a more reliable test of TFO delivery systems.

In this study we describe ‘radioprinting’, a new method for detection of triplex formation. The method is based on the use of TFOs labeled with  $^{125}\text{I}$ . Decay of  $^{125}\text{I}$  produces DNA strand breaks in the target duplex that are located within a few base pairs from the decay site (12–14). The presence of  $^{125}\text{I}$ -induced breaks in the target sequence proves the existence of the triplex at the time of  $^{125}\text{I}$  decay. As a model we used the plasmid pCR3HPRT containing the triple helix-forming polypurine-polypyrimidine region of the human hypoxanthine-guanine phosphoribosyl-transferase (HPRT) gene (13). A triplex was preformed on the plasmid and then delivered into cells by lipofection. Others previously demonstrated that triplexes preformed on a linear DNA molecule are stable inside cells (15). Here, by using radioprinting, we show that triplexes are stable inside cells for at least 48 h on covalently closed plasmid DNA. Based on these data we propose a new method for labeling of intact plasmid DNA via TFOs.

## MATERIALS AND METHODS

### Plasmids

Plasmid pCR3HPRT containing the triple helix-forming polypurine-polypyrimidine region of the human HPRT gene was constructed by inserting the PCR-amplified fragment into pCR3 vector (Invitrogen, Carlsbad, CA), as previously

\*To whom correspondence should be addressed. Tel: +1 301 496 8308; Fax: +1 301 496 0114; Email: igorp@helix.nih.gov

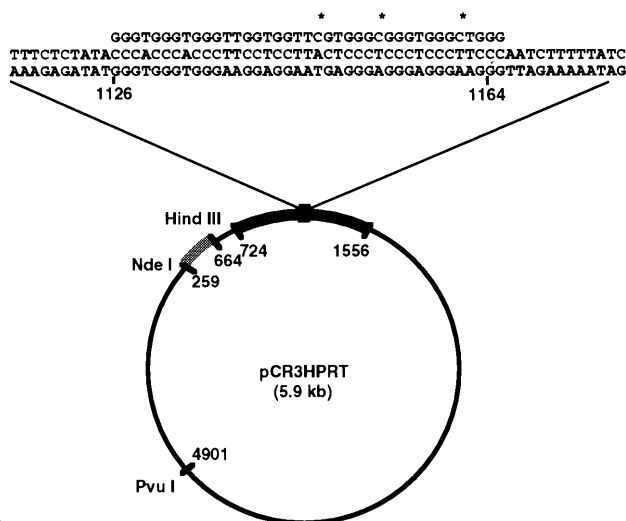


**Figure 1.** Scheme of the pCR3HPRT plasmid. The 833 bp PCR fragment cloned into the pCR3 vector (positions 724–1556) is shown in bold. (Inset) The target sequence along with the TFO. Positions of  $^{125}\text{I}$ -labeled dC residues are marked with stars. The probe for Southern hybridization cut from the plasmid by restriction enzymes *Hind*III and *Nde*I is shown in gray.

described (13). Prior to use, the supercoiled plasmid was relaxed with topoisomerase I (Promega, Madison, WI). Plasmid pCMV-sport- $\beta$ -gal containing the  $\beta$ -galactosidase gene was purchased from Gibco BRL. All plasmids were purified by centrifugation through a CsCl gradient.

### Triplex-forming oligonucleotides (TFOs)

Oligodeoxyribonucleotides were synthesized on an ABI-394 DNA synthesizer (Applied Biosystems, Foster City, CA) followed by purification by PAGE as previously described (12–14). The template oligonucleotide was biotinylated using BioTEG modifiers (Glen Research, Sterling, VA). The phosphodiester TFO was labeled with [ $^{125}\text{I}$ ]dCTP at the C5 position of three cytosines (marked with stars in Fig. 1) by the primer extension method (13,14). The product TFO was estimated to have 1.5  $^{125}\text{I}$  per oligonucleotide. The fluorescein (FITC)-labeled TFO was synthesized using FITC modifiers (Glen Research).

### Triplex formation and stability

[ $^{125}\text{I}$ ]TFO or FITC-TFO were mixed with relaxed plasmid pCR3HPRT in a TMSp buffer containing 50 mM Tris-HCl, pH 8, 10 mM MgCl<sub>2</sub>, 0.1 mM spermidine and 16  $\mu\text{M}$  coralyne chloride (Sigma, St Louis, MO) (16–18). Aliquots of the samples were analyzed in a 2% agarose gel at 10°C using TAE buffer containing 3 mM MgAc as an electrode buffer for 1 h at 60 V. Gels were analyzed with a BAS 1500 Bio-Imaging Analyzer (Fuji, Tokyo, Japan) or FluorImager (Molecular Dynamics, Sunnyvale, CA).

### Cell line and culture conditions

The human cervix epithelial carcinoma HeLa cell line (CCL2; ATCC, Manassas, VA) was grown in monolayer in Dulbecco's

modified Eagle's minimum essential medium (DMEM), supplemented with 0.1 mM non-essential amino acids and 10% fetal bovine serum (FBS), purchased from BioWhittaker (Walkersville, MD). All procedures were done according to ATCC recommendations.

### DNA/liposome complexes

For transfection experiments we used DMRIE-C liposomes (Gibco BRL, Gaithersburg, MD). Five microliters of DMRIE-C (initial concentration 2 mg/ml) was diluted in 45  $\mu\text{l}$  OptiMEM medium (Gibco BRL). Three micrograms of plasmid DNA (or plasmid/TFO triplex) was diluted in OptiMEM to 50  $\mu\text{l}$ . Fifty microliters of the liposome solution were mixed with DNA solution. The mixture was left for 20–30 min at room temperature before further use.

### Transfection experiments

Cells were grown in 6-well plates to 70–80% confluency and washed with OptiMEM medium. Then 900  $\mu\text{l}$  of OptiMEM was added to each well and the cells were placed in a CO<sub>2</sub> incubator at 37°C until further use. DNA/DMRIE-C complexes (100  $\mu\text{l}$ ) were added to each well. The cells were incubated for 5 h, washed with DMEM containing 3 mM EDTA and then post-incubated in DMEM medium for the desired time. After the incubation was completed, the cells were trypsinized, collected, frozen and stored at  $-70^\circ\text{C}$  for 60 days to accumulate  $^{125}\text{I}$  decay. Cells precipitated by centrifugation and medium were counted in a  $\gamma$  scintillation counter (Auto-Gamma 5650; Packard, Downers Grove, IL) to determine cellular uptake of the initial input dose of radioactivity (19).

To study the transfection efficiency with pCMV-sport- $\beta$ -gal/DMRIE-C, the transfected cells were fixed in fixative solution (2% formaldehyde, 0.2% glutaraldehyde in PBS) and stained with a  $\beta$ -gal staining kit (Invitrogen). The blue cells were counted microscopically (Karl Zeiss, Oberkochen, Germany). To check the viability of transfected cells, we stained the cells with trypan blue and counted the number of dead and surviving cells microscopically. Fluorescent and confocal microscopy and autoradiography were performed as previously described (19).

### DNA breaks analysis

pCR3HPRT plasmid DNA was extracted from cells and nuclei, following the modified Hirt extraction procedure (20). Shortly afterwards, the cell pellet was resuspended in 0.5 ml Hirt buffer (0.6% SDS, 10 mM EDTA, 10 mM Tris-HCl) and was left to stand for 10 min with occasional agitation. The content was added to a microtube containing 150  $\mu\text{l}$  of 5 M NaCl. The tube was placed on ice overnight, then spun for 10 min to precipitate chromosomal DNA. One hundred micrograms of yeast RNA and 100  $\mu\text{g}$  of proteinase K were added to the supernatant and the tube was incubated for 1–2 h at 50°C. DNA was extracted twice with equal volumes of phenol/chloroform and then once with chloroform. The supernatant from the last extraction was placed in a microtube containing 150  $\mu\text{l}$  of 10 M ammonium acetate and 700  $\mu\text{l}$  of isopropanol. The tube was inverted several times and spun for 30 min in a microcentrifuge. The pellet was dried and resuspended in 50  $\mu\text{l}$  of TE buffer, then precipitated with ethanol, washed with 70% cold ethanol and spun again. The dried pellet was resuspended in TE buffer.

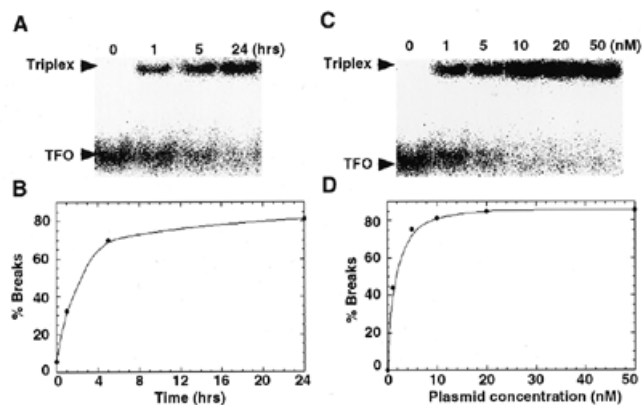


**Figure 2.** Kinetics of triplex formation (A and B) and equilibrium binding (C and D). (A) One nanomolar [ $^{125}$ I]TFO and 10 nM plasmid pCR3HPRT were incubated at 37°C in TMSp buffer for different periods of time (0–24 h). (C) Overnight incubation at 37°C was performed with 1 nM [ $^{125}$ I]TFO and different concentrations of plasmid (0–50 nM). The arrows show the triplex and TFO positions. (B and D) Percent of breaks calculated as the ratio of the intensity of the upper triplex band to the total intensity of the bands in the lane is plotted against time and plasmid concentration

Plasmid DNA was electrophoresed through a 1% agarose gel and transferred to a Genescreen hybridization membrane (NEN Life Science Products, Boston, MA). The membrane was hybridized with the shorter (405 bp, Fig. 1) *HindIII–NdeI* fragment of plasmid pCR3HPRT  $^{32}$ P-labeled with an oligo-labeling kit (Pharmacia Biotech, Piscataway, NJ) following the manufacturer's instructions and visualized with a BAS 1500 Bio-Imaging Analyzer.

## RESULTS

### Triplex formation *in vitro*

In this study we used as a model a triplex-forming sequence from the human HPRT gene that has been described before (13,14). A map of plasmid pCR3HPRT containing the 832 bp insert from the human HPRT gene intron A (13,21) along with the triplex-forming sequence and purine motif TFO are shown in Figure 1. The TFO was labeled with [ $^{125}$ I]dCTP by a primer extension method as previously described (12). Plasmid (10 nM) was incubated with [ $^{125}$ I]TFO (1 nM) at 37°C for 1, 5 and 24 h in TMSp buffer. As a control, an aliquot of the mixture was not incubated but instead kept on ice (0 h). Triplex formation was monitored by gel shift assay (12,22) and the results of the kinetics of binding experiment are shown in Figure 2A and B. At 10 nM concentration 50% binding of [ $^{125}$ I]TFO to the plasmid occurred only after 4 h incubation at 37°C. As expected, no binding occurred in the 0 h control (Fig. 2B). Such slow kinetics of formation for purine motif triplexes have been observed before (23).

An equilibrium binding experiment with different concentrations of the plasmid and overnight incubation at 37°C is shown in Figure 2C and D. At 1 nM concentration of both plasmid and TFO ~50% of the TFO was bound to the plasmid. This shows

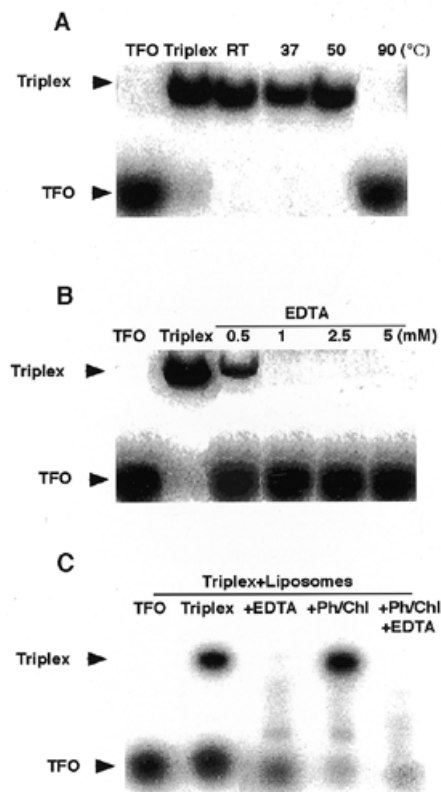


**Figure 3.** Triplex stability *in vitro*. (A) The preformed triplex was diluted in a buffer containing 0.5 mM  $MgCl_2$  and aliquots were incubated at room temperature, 37 and 50°C for 30 min and at 90°C for 1 min. (B) The preformed triplex was diluted in a buffer without  $MgCl_2$  (the final concentration of magnesium was 1 mM) and aliquots were incubated with 0.5, 1, 2.5 and 5 mM EDTA for 10 min at 37°C. (C) The preformed triplex was mixed with DIMRIE-C liposomes as described in Materials and Methods. The complex was incubated with 10 mM EDTA for 10 min at 37°C. The last two samples are shown after phenol/chloroform (Ph/Chl) extraction. The arrows show the positions of triplex and TFO.

that binding of the selected TFO occurs even at subnanomolar concentrations, which is important, since the concentration of [ $^{125}$ I]TFO that could be delivered into cells was limited to reduce non-specific radiation damage.

### Triplex stability *in vitro*

To study the stability of the triplex *in vitro*, an aliquot of the preformed triplex was diluted 10 times in 20 mM Tris–HCl, 20 mM NaCl, 0.5 mM  $MgCl_2$  buffer and kept overnight at room temperature. Aliquots of the diluted sample were also incubated at 37 and 50°C for 30 min and at 90°C for 1 min. Figure 3A shows that the triplexes remained stable under all the conditions; only after heating at 90°C was complete dissociation observed. This showed that the triplex remains stable after dilution and incubation at elevated temperatures.

In the next experiment, aliquots of preformed triplex were diluted in 20 mM Tris–HCl, 20 mM NaCl buffer without

MgCl<sub>2</sub> (the final concentration of magnesium was 1 mM) and incubated with 0.5, 1, 2.5 and 5 mM EDTA for 10 min at 37°C. As shown in Figure 3B, 60% of the triplex incubated with 0.5 mM EDTA dissociated and all the triplexes incubated with higher concentrations of EDTA dissociated completely.

We used 0.5 mM EDTA to find the triplex stability dependence on time of incubation at 37°C. About 60% of triplexes dissociated immediately after EDTA was added and the percentage remained stable during 1 h incubation (data not shown). This result indicates that magnesium is absolutely required for stability of the triplex; addition of an equimolar equivalent of EDTA results in immediate dissociation of the triplexes.

Since the triplexes were to be delivered into cells with liposomes, it was important to know their stability within liposome complexes. The experiment presented in Figure 3C addressed this issue. Preformed triplexes were mixed with DIMRIE-C liposomes as described in Materials and Methods. Aliquots were incubated at 37°C for 10 min in the presence or absence of EDTA. Clearly, triplexes remained stable within the liposome complex but addition of EDTA caused their dissociation. To remove liposomes prior to electrophoresis we used phenol extraction, which by itself could disrupt triplexes. Interestingly, even loaded directly with liposomes, DNA entered the gel in the normal way. This means that cationic liposome complexes dissociate in the electric field during electrophoresis.

### Radioprinting *in vitro*

We first tested radioprinting under conditions where triplex formation could be proved by conventional methods like the gel shift assay. A series of samples with different percents of triplex formation was prepared. All samples contained 80 nM plasmid pCR3HPRT and 8, 20, 40, 64 or 80 nM [<sup>125</sup>I]TFO. Gel shift analysis showed that all the added [<sup>125</sup>I]TFO was bound to plasmids after overnight incubation at 37°C (data not shown). Therefore, the percents of plasmids carrying TFO in the samples were 10, 25, 50, 80 and 100%, respectively. The samples were frozen for 60 days to accumulate <sup>125</sup>I decay, then thawed, cut with *Pvu*I restriction enzyme and analyzed in a 1% agarose gel stained with ethidium bromide (Fig. 4A). Breaks at the triplex-forming sequence of pCR3HPRT produced by decay of <sup>125</sup>I in [<sup>125</sup>I]TFO along with *Pvu*I cleavage gave rise to two fragments of 3.74 and 2.16 kb (Figs 1 and 4A). The intensity of the bands corresponding to these fragments increases with the increase in the percent of triplexes formed on the plasmid.

The bands from a gel similar to that shown in Figure 4A were transferred to a nylon membrane and hybridized with the <sup>32</sup>P-labeled *Hind*III-*Nde*I probe (Figs 1 and 4B). The probe hybridized only with the 2.15 kb fragment. The intensity of the band corresponding to that fragment increases with increasing percentage of triplex. The percent of breaks calculated as intensity of the decay-produced bands to the total intensity of all bands in the lanes is plotted against the percentage of triplexes in Figure 4C. The [<sup>125</sup>I]TFO-produced breaks are directly proportional to the percent of triplexes on the plasmid. Our data show that radioprinting, i.e. measuring [<sup>125</sup>I]TFO-produced breaks either by direct staining with ethidium bromide or by Southern hybridization, can be used to quantitatively determine the amount of [<sup>125</sup>I]TFO bound to a plasmid based on the known number of breaks. The slightly lower values for the percentage of breaks in the hybridization experiments as

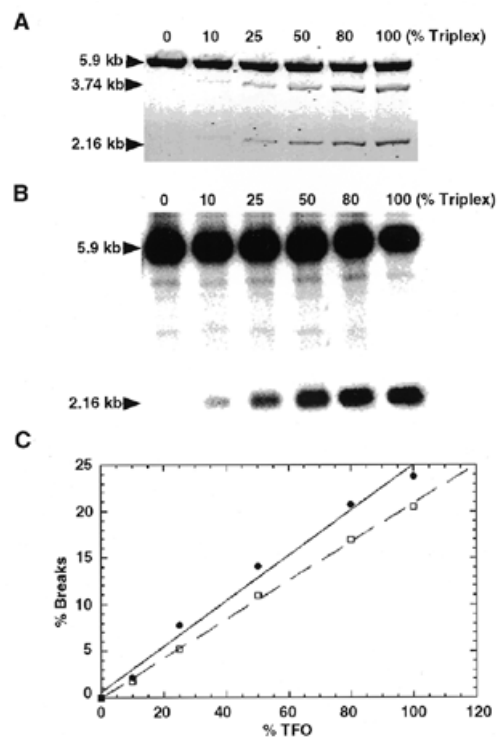


**Figure 4.** Triplex radioprinting *in vitro*. (A) Electrophoresis in agarose gel with ethidium bromide. Triplexes were preformed with different concentrations of [<sup>125</sup>I]TFO, then frozen and kept at -70°C for <sup>125</sup>I decay accumulation. The percent of the plasmid carrying TFO in the samples is shown at the top. The positions of the bands are shown with arrows with the corresponding length in kb. (B) Southern blot of a gel with the same samples as in (A) hybridized with a <sup>32</sup>P-labeled *Hind*III-*Nde*I probe. The probe hybridizes only to the shorter fragment. (C) Percent of double-strand DNA breaks versus percent of bound TFO. Percent of breaks was calculated as the ratio of the sum of the intensities of the two shorter bands in the case of the ethidium stained gel (circle) and the intensity of the single shorter band in the case of the Southern blot (square) to the total intensities of the bands in lanes.

compared with the ethidium bromide staining can be attributed to the weaker probe hybridization with the shorter fragment.

The maximum number of DNA breaks in the samples with 100% triplex formation was 23.7% as measured with ethidium bromide staining and 20.6% as determined by Southern hybridization. Since each TFO contained on average 1.5 <sup>125</sup>I atoms and for 60 days only half of them decayed the efficiency in terms of double-strand breaks per decay can be estimated as 40%, which is in good agreement with our previously published data for the purine motif triplex (13,14).

### Triplex delivery into cells

To deliver plasmid DNA into HeLa cells we used DMRIE-C liposomes. After optimization of transfection conditions with plasmid pCMV-sport- $\beta$ -gal, we obtained 60% transfection efficiency, i.e. 60% of transfected cells expressed the  $\beta$ -galactosidase gene and became blue after staining with a  $\beta$ -gal Staining

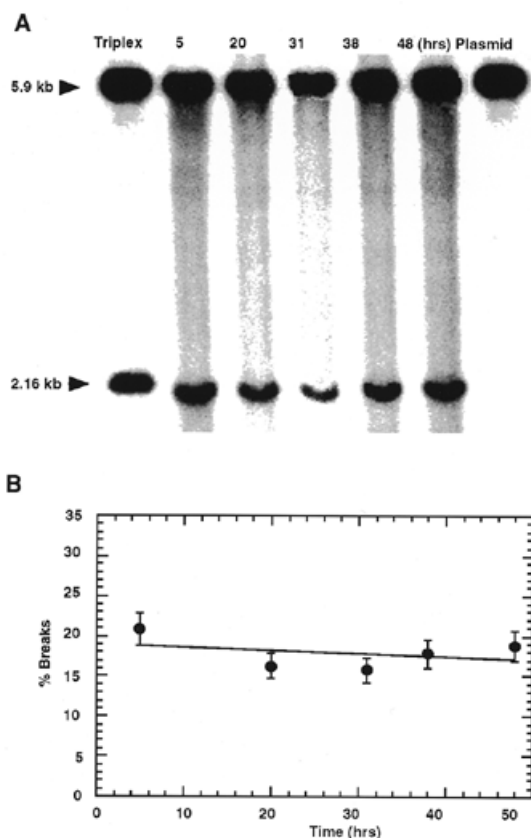


**Figure 5.** Triplex radioprinting in cells. (A) Southern blot of Hirt extracts from HeLa cells that had been transfected with preformed triplexes ( $[^{125}\text{I}]\text{TFO}/\text{pCR3HPRT}$ ). Cells were incubated with triplexes for 5 h and post-incubated for 17–43 h, then frozen and stored at  $-70^\circ\text{C}$  to accumulate  $^{125}\text{I}$  decay. The recovered plasmid was cut with *PvuI*. The blot was hybridized with a  $^{32}\text{P}$ -labeled *HindIII*–*NdeI* probe. As a positive control we used triplex that was stored in a test tube without delivery into cells (Triplex). As a negative control we used plasmid pCR3HPRT delivered into cells and Hirt extracted (Plasmid). (B) Percent double-strand plasmid DNA breaks versus time of incubation of the cells with preformed triplexes.

Kit. Staining with trypan blue showed that almost 90% of cells survived transfection (not shown). When preformed  $[^{125}\text{I}]\text{TFO}/\text{pCR3HPRT}$  triplexes were delivered into cells, 30% of the radioactivity was associated with the cell pellet after 5 h incubation.

### Triplex radioprinting in cells

To analyze intracellular triplex stability, cells were transfected with preformed triplex (equal amounts of plasmid pCR3HPRT and  $[^{125}\text{I}]\text{TFO}$ ) were used for triplex formation) using DMRIE-C liposomes. Cells were incubated with liposomes for 5 h and then washed with DMEM containing 3 mM EDTA. As shown above, the presence of EDTA would remove TFO from the plasmids that remained outside the cells even within the complexes with liposomes (Fig. 3C). After a DMEM + EDTA wash cells were post-incubated in DMEM for 20, 31, 38 or 48 h. Then cells were collected and frozen for 60 days. After thawing,

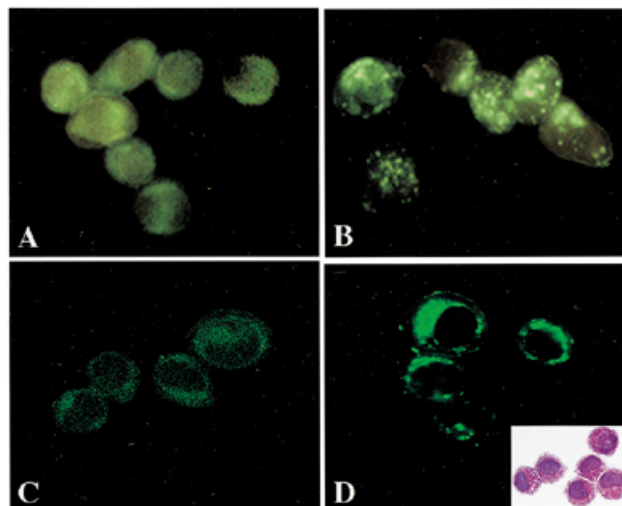


**Figure 6.** Distribution of triplexes inside cells. Fluorescent (A and B) and confocal (C and D) analysis of HeLa cells transfected with preformed triplexes (FITC–TFO/pCR3HPRT plasmid) complexed with DMRIE–C liposomes (A and C). As a control, we transfected cells with FITC–TFO/DMRIE–C (B and D). (Inset) Staining with hematoxylin and eosin. Magnification 100 $\times$ .

plasmid DNA was extracted, as described above, cut with *PvuI* restriction enzyme and analyzed in 1% agarose gels followed by Southern hybridization with the *HindIII*–*NdeI* probe to detect  $[^{125}\text{I}]\text{TFO}$  induced breaks. The results are shown in Figure 5A and B. Lane 1 shows the control triplex that had been frozen in a test tube for the same period of time. All of the analyzed samples contained approximately the same amount of breaks, i.e. ~20%. This means that inside the living cells triplexes remained stable for at least 48 h and there was no significant dissociation of TFO.

### Distribution of TFO/plasmid complexes inside cells

For this experiment we used FITC-labeled TFO to visualize plasmid/TFO complexes inside cells. Cells were transfected with preformed FITC–TFO/pCR3HPRT triplexes using DMRIE–C liposomes. As a control, we transfected the cells with FITC–TFO alone using the same liposomes. Fluorescent (Fig. 6A and B) and confocal (Fig. 6C and D) microscopy showed that FITC-labeled triplexes (Fig. 6A and C) were distributed throughout the cells and could be found both in cytoplasm and nuclei. In contrast, FITC–TFO alone (Fig. 6B and D) was concentrated in bright grains in the cytoplasm. This indicates that the liposome formulation that is optimal for plasmid delivery is not adequate for the delivery of short TFO and after penetration into cells most of the TFO remained associated with liposomes. Earlier we showed that when delivered with a liposome formulation that is optimal for short oligonucleotides, TFO was liberated from the liposomes to the cytoplasm and very soon was concentrated exclusively in the nucleus (19). Combined with the fact that TFO was still bound to plasmids, this experiment shows that plasmid vectors inside the cells, unlike short oligonucleotides, do not concentrate predominantly in nuclei.

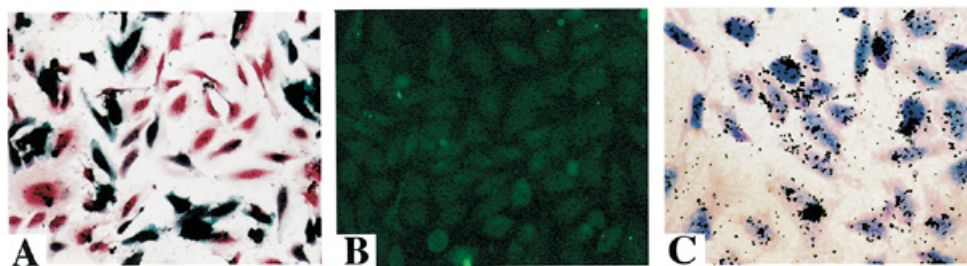


**Figure 7.** Transfection of HeLa cells grown on a slide surface with: (A) plasmid pCMV-sport- $\beta$ -gal, staining with  $\beta$ -gal staining kit, counterstaining with nuclear fast red; (B) preformed FITC-TFO/pCR3HPRT triplexes; (C) preformed [ $^{125}\text{I}$ ]TFO/pCR3HPRT triplexes (autoradiography), counterstaining with 1% methylene blue and red counterstain C. Magnification 40 $\times$ .

Hematoxylin and eosin staining of the cells was also used in this experiment to visualize nuclei (Fig. 6, inset).

In addition, we found fluorescent signals in almost all the cells, while detection of delivery with the conventional method using a marker gene ( $\beta$ -galactosidase) revealed expression of the gene in only half of the cell population (Fig. 7A and B). Autoradiography confirms delivery of the [ $^{125}\text{I}$ ]TFO/pCR3HPRT triplexes to all the cells (Fig. 7C). This illustrates that TFO-mediated labeling of plasmid vectors could be used for optimization of plasmid vector delivery in gene therapy protocols.

## DISCUSSION

We describe 'radioprinting', a new method for detection of binding of radiolabeled oligonucleotides to DNA targets. The method is based on analysis of DNA breaks induced by a highly localized Auger effect from the decay of such radionuclides as  $^{125}\text{I}$ ,  $^{123}\text{I}$ ,  $^{111}\text{In}$  and others. Earlier we described radioprobeing, a method that detects conformational changes in DNA structure by measuring the distribution of Auger emitter-induced breaks with single nucleotide resolution (14). Radioprinting can be considered as a low resolution form of radioprobeing. To document triplex formation we simply need to find breaks in the target sequence, not their spatial distribution. Although with the development of methods of analysis of the break distribution *in vivo* more precise than Southern blotting we may be able to obtain information on the conformation of DNA triplex inside cells. Better methods could include, for example, ligation-mediated PCR (24).

The experiments described in this paper were performed with commercially available [ $^{125}\text{I}$ ]dCTP and can be easily repeated in any laboratory. The drawback of using  $^{125}\text{I}$  is its 60 days half-life, which requires freezing of the samples for decay accumulation. The use of Auger emitters with shorter half-lives, for example  $^{123}\text{I}$  (13 h),  $^{111}\text{In}$  (2.6 days) and  $^{67}\text{Ga}$  (78 h), would allow considerably shortened radioprinting procedures and avoid cell freezing (25,26). The metallic Auger emitters can be attached to the TFO through chelators, as previously described (26–28). The shorter half-life Auger emitters could also be applied for radioprinting experiments in animal models. In

principle, the radioprinting can be extended to detect interaction of a target DNA or RNA sequence with any Auger emitter-labeled ligand: proteins, nucleic acids, peptides, chemicals and other low molecular weight compounds.

Radioprinting, as defined above, allowed us for the first time to show that triplexes preformed on covalently closed circular DNA remained stable inside cells for at least 48 h. For this study we used a phosphodiester TFO with a dissociation constant in the nanomolar range. The low dissociation constant is important for the radiolabeled TFO in order to minimize non-specific radiation damage to DNA and cells. The use of backbone and/or base modifications that stabilize the triplex would allow a further reduction in radioactivity used in radioprinting experiments (6). Stabilization of the TFO is likely to be especially important for *in vivo* experiments.

The persistent stability of triplexes makes them convenient labeling agents for plasmid DNA. Plasmids are used as DNA vectors in various applications. Labeling them directly for imaging purposes is time consuming and the introduced labeling groups could become substrates for the repair system. Unlike intact circular plasmid DNA, TFOs can be labeled *in vitro* not only with fluorescent agents but also with diagnostic radioisotopes. For example,  $^{18}\text{F}$ -labeled oligonucleotides were recently successfully used for biodistribution studies using positron emission tomography (PET) (29). Labeling with radioisotopes such as  $^{124}\text{I}$ ,  $^{111}\text{In}$  and  $^{99\text{m}}\text{Tc}$  (26–28), used for imaging with PET and  $\gamma$  cameras, or with gadolinium, for imaging with MRI, we propose this new method as a non-invasive way to study the biodistribution of plasmids *in vivo*.

## REFERENCES

- Hélène, C. (1991) *Anti-Cancer Drug Des.*, **6**, 569–584.
- Frank-Kamenetskii, M.D. and Mirkin, S.M. (1995) *Annu. Rev. Biochem.*, **64**, 65–69.
- Giovannangeli, C. and Hélène, C. (1997) *Antisense Nucleic Acids Drug Dev.*, **7**, 413–421.
- Plum, G.E. and Pilch, D.S. (1995) *Annu. Rev. Biophys. Biomol. Struct.*, **24**, 319–350.
- Neilsen, P.E. (1995) *Annu. Rev. Biophys. Biomol. Struct.*, **24**, 167–183.
- Chan, P.P. and Glazer, P.M. (1997) *J. Mol. Med.*, **75**, 267–282.
- Giovannangeli, C., Diviacco, S., Larbrousse, V., Gryaznov, S., Charneau, P. and Hélène, C. (1997) *Proc. Natl Acad. Sci. USA*, **94**, 79–84.

8. Belousov, E.S., Afonina, I.A., Kutuyavin, I.V., Gall, A.A., Reed, M.W., Gamper, H.B., Wydro, R.M. and Meyer, R.B. (1998) *Nucleic Acids Res.*, **26**, 1324–1328.
9. Guieysse, A.-L., Praseuth, D., Grigoriev, M., Harel-Bellan, A. and Hélène, C. (1996) *Nucleic Acids Res.*, **24**, 4210–4216.
10. Majumdar, A., Khorlin, A., Dyatkina, N., Lin, F.-L.M., Powel, J., Liu, J., Fei, Z., Khripine, Y., Watanabe, K.A., George, J., Glaser, P.M. and Seidman, M.M. (1998) *Nature Genet.*, **20**, 212–214.
11. Wang, G., Seidman, M.M. and Glazer, P.M. (1996) *Science*, **271**, 802–805.
12. Panyutin, I.G. and Neumann, R.D. (1994) *Nucleic Acids Res.*, **25**, 883–887.
13. Panyutin, I.G. and Neumann, R.D. (1996) *Acta Oncol.*, **36**, 817–824.
14. Panyutin, I.G. and Neumann, R.D. (1997) *Nucleic Acids Res.*, **25**, 883–887.
15. Debin, A., Malvy, C. and Svinarchuk, F. (1997) *Nucleic Acids Res.*, **25**, 1965–1974.
16. Lee, J.S., Latimer, L.J.P. and Hampel, K.J. (1993) *Biochemistry*, **32**, 5591–5597.
17. Belousov, E.S., Afonina, I.A., Podyminogin, M.A., Gamper, H.B., Reed, M.W., Wydro, R.M. and Meyer, R.B. (1997) *Nucleic Acids Res.*, **25**, 3440–3444.
18. Lampe, J.N., Kutuyavin, I.V., Rhinehart, R., Reed, M.W., Meyer, R.B. and Gamper, H.B., Jr (1997) *Nucleic Acids Res.*, **25**, 4123–4131.
19. Sedelnikova, O.A., Panyutin, I.G., Thierry, A.R. and Neumann, R.D. (1998) *J. Nucl. Med.*, **39**, 1412–1418.
20. Hirt, B. (1967) *J. Mol. Biol.*, **36**, 365–369.
21. Edwards, A., Voss, H., Rice, P., Civitello, A., Stegemann, J., Schwager, C., Zimmermann, J., Erfle, H., Caskey, C.T. and Ansorge, W. (1990) *Genomics*, **6**, 593–608.
22. Cooney, M., Czernuszewicz, G., Postel, E.H., Flint, S.J. and Hogan, M.E. (1988) *Science*, **241**, 456–459.
23. Vasquez, K.M., Wenzel, T.G., Hogan, M.E. and Wilson, J.H. (1995) *Biochemistry*, **34**, 7243–7251.
24. Pfeifer, G.P. and Tornaletti, S. (1997) *Methods Companion Methods Enzymol.*, **11**, 189–196.
25. Martin, R.F., Allen, B.J., d’Cunha, G., Gibbs, R., Murray, V. and Pardee, M. (1988) In Baverstock, K.F. and Charlton, D.E. (eds), *DNA Damage by Auger Emitters*. Taylor & Francis, New York, NY, pp. 55–68.
26. Hnatowich, D.J., Mardirossian, G., Fogarasi, M., Sano, T., Smith, C.L., Cantor, C.R., Rusckowski, M. and Winnard, P., Jr (1996) *J. Pharmacol. Exp. Ther.*, **276**, 326–334.
27. Dewanjee, M.K., Ghafouripour, A.K., Kapadvanjwala, M., Dewanjee, S., Serafini, A.N., Lopes, D.N. and Sfakianakis, G.N. (1994) *J. Nucl. Med.*, **35**, 1054–1063.
28. Sahu, S.K., Kassis, A.I., Makrigiorgos, G.M., Baranowska-Kortilewicz, J. and Adelstein, S.J. (1995) *Radiat. Res.*, **141**, 193–198.
29. Tavitian, B., Terrazino, S., Kühnast, B., Marzabal, S., Stettler, O., Dollé, F., Deverre, J.-R., Jobert, A., Hinnen, F., Bendriem, B., Crouzel, C. and Giambraadino, L.D. (1998) *Nature Med.*, **4**, 467–471.